Organic & Biomolecular Chemistry

Accepted Manuscript

This article can be cited before page numbers have been issued, to do this please use: P. Mai, G. Zocher, T. Stehle and S. Li, *Org. Biomol. Chem.*, 2018, DOI: 10.1039/C8OB02037J.

ROYAL SOCIETY OF CHEMISTRY

rsc.li/obc

View Article Online
DOI: 10.1039/C8OB02037J

Organic & Biomolecular Chemistry

PAPER

Structure-based protein engineering enables prenyl donor switching of a fungal aromatic prenyltransferase

Received 00th xxx 20xx,
Accepted 00th xxx 20xx

DOI: 10.1039/x0xx00000x

www.rsc.org/

Peter Mai,[a] Georg Zocher,[b] Thilo Stehle,*[b] and Shu-Ming Li*[a]

Microorganisms provide valuable enzyme machineries to assemble complex molecules. Fungal prenyltransferases (PTs) typically catalyse highly regiospecific prenylation reactions that are of significant pharmaceutical interest. While the majority of PTs accepts dimethylallyl diphosphate (DMAPP), very few such enzymes can use geranyl diphosphate (GPP) or farnesyl diphosphate (FPP) as donors. This catalytic gap prohibits the wide application of PTs for structural diversification. Structure-guided molecular modelling and site-directed mutagenesis of FgaPT2 from *Aspergillus fumigatus* led to the identification of the gatekeeping residue Met328 responsible for the prenyl selectivity and sets the basis for creation of GPP- and FPP-accepting enzymes. Site-saturation mutagenesis of the gatekeeping residue at position 328 in FgaPT2 revealed that the size of this side chain is the determining factor for prenyl selectivity, while its hydrophobicity is crucial for allowing DMAPP and GPP to bind.

Introduction

Natural products from plants and microorganisms are important sources for drugs.[1-3] Diverse enzymes are involved in the biosynthesis of these compounds.[4] Prenyltransferases (PTs) catalyse transfer reactions of prenyl (nxC5) moieties onto aliphatic or aromatic acceptors.[5] Nature provides an impressive repertoire of functionally versatile PTs in diverse metabolic pathways. Prenylation often increases the hydrophobic character of the target structures and enables or enhances their interaction with biomolecules. For example, protein prenylation can be an essential posttranslational modification for specific protein-protein and protein-membrane interactions in cell signalling cascades across species.[6] In bacteria, special peptide pheromones obtain their functionality as signalling molecules by prenylation of tryptophan residues.[7,8] Discovery of prenylated t-RNA underlines the crucial role of nucleic acid PTs to impact translation processes.[9]

Over the last two decades, progress in genome sequencing and mining enables prediction of metabolites from genetic potentials. The rich source of biologically active metabolites in ascomycetous fungi implied tremendous efforts in structural and mechanistic investigations of enzyme machineries, as exemplified by the biosynthesis of indole alkaloids.[10] Fungal PTs are found either to commit the starting point of biosynthetic pathways or to tailor assembled scaffolds, providing particular benefits to the structural diversity of metabolites.[11] To date, about fifty PTs from fungi and bacteria belonging to the dimethylallyltryptophan synthase (DMATS) superfamily have been characterized biochemically.[5] Crystal structures of the DMATS-type PTs show a conserved PT barrel fold composing of five ααββ repeating units with ten circularly arranged antiparallel β-strands surrounded by ten α-helices. This ABBA-type architecture was initially observed for the bacterial PT NphB[12] and for the fungal *C4*-dimethylallyltryptophan synthase FgaPT2, although the two enzymes share little sequence similarity with each other.[13] DMATS-type PTs usually use dimethylallyl diphosphate (DMAPP, C5) as a prenyl donor and catalyse metal ion-independent Friedel-Crafts alkylation on their aromatic substrates. The enzymatically generated dimethylallyl carbocation is attacked by electron-rich atoms, *e.g.* C-C double bond, N-, or O-atom, at its C-1 or C-3, resulting in regular and reverse prenylation, respectively.[5]

Biochemical investigations of DMATS-type PTs revealed clear promiscuity towards aromatic acceptors. However, the majority of these PTs displays high specificity for DMAPP and low or no activity towards longer donors like geranyl diphosphate (GPP, C10) or farnesyl diphosphate (FPP, C15). VrtC and TleC are the two examples of the DMATS superfamily that require GPP for activity.[14] A minority of DMATSs, *e.g.* AtaPT, MpnD, TleC, BAE61387, and AstPT, can utilize a range of prenyl donors.[15-18] The high specificity for prenyl donor limits their application for structural diversification.

[a] *Institut für Pharmazeutische Biologie und Biotechnologie, Philipps-Universität Marburg, Robert-Koch-Straße 4, 35037 Marburg, Germany. E-Mail: shuming.li@staff.uni-marburg.de*
[b] *Interfakultäres Institut für Biochemie, Eberhard Karls Universität Tübingen, Tübingen 72076, Germany. E-Mail: thilo.stehle@uni-tuebingen.de*
[c] *† Electronic Supplementary Information (ESI) available: Primers, ^{1}H NMR spectrum of **3** with assignments, MS data, and determination of kinetic parameters (PDF). See DOI: 10.1039/x0xx00000x*

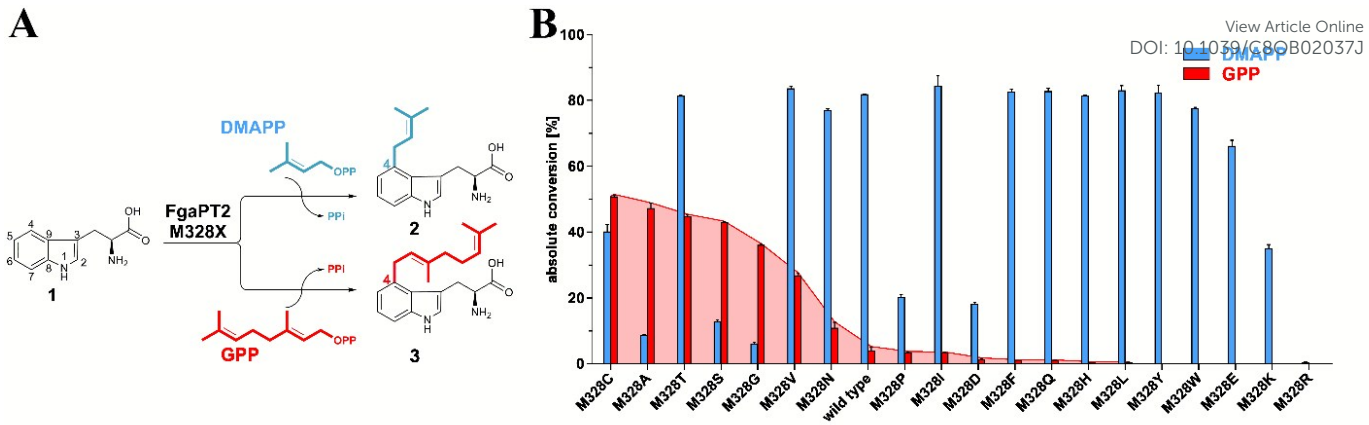

Fig. 1 Prenylation of L-tryptophan by FgaPT2 and its M328 mutants in the presence of DMAPP (blue) and GPP (red). A) Enzyme products and B) absolute conversion yields

The particular importance and necessity of GPP-, and FPP-accepting enzymes as biocatalytic tools led us to perform a directed evolution study. The selected tryptophan PT FgaPT2 from *Aspergillus fumigatus* utilizes DMAPP as the natural prenyl donor and catalyses the *C4*-prenylation of L-tryptophan (**1**) to yield 4-dimethylallyltryptophan (**2**)[19] (Fig. 1A). The availability of structures for several DMATS-type PTs such as FgaPT2,[13] FtmPT1,[20] CdpNPT,[21] AnaPT,[22] AtaPT,[15] TleC, and MpnD[16] provides a molecular basis for understanding the reaction mechanisms and enables structure-based protein design and engineering.

In this study, we genetically engineered the PT FgaPT2 based on its crystal structure[13] by molecular modelling and identified a gatekeeping residue for the prenyl donor specificity. Furthermore, site-saturation mutagenesis at the gatekeeping residue provides insights into the molecular effects of the interactions between various prenyl donors and altering amino acids.

Results and discussion

Methionine 328 in FgaPT2 controls the prenyl donor gateway

To confirm the preference for DMAPP observed in a previous study, we synthesized chemically DMAPP, GPP and FPP[23] and confirmed their integrity by NMR analysis (Figs. S1 – S6). FgaPT2 (10 µg) was then incubated with 1mM **1** in the presence of 1mM DMAPP, GPP or FPP at 37 C for 90 min. The reaction mixtures were subsequently analysed by LC-MS. **2** with a conversion of 81.7% was detected in the incubation mixture with DMAPP. When GPP was used as a prenyl donor, the geranylated product **3** showed a drastically reduced conversion of only 3.8% (Figure 1B and Figure 2) and no conversion at all when **1** is incubated with FgaPT2 in the presence of FPP. (Figure 3)

Structure-based molecular modelling led to the identification of Met328 in FgaPT2 as a putative gatekeeping residue. The side chain

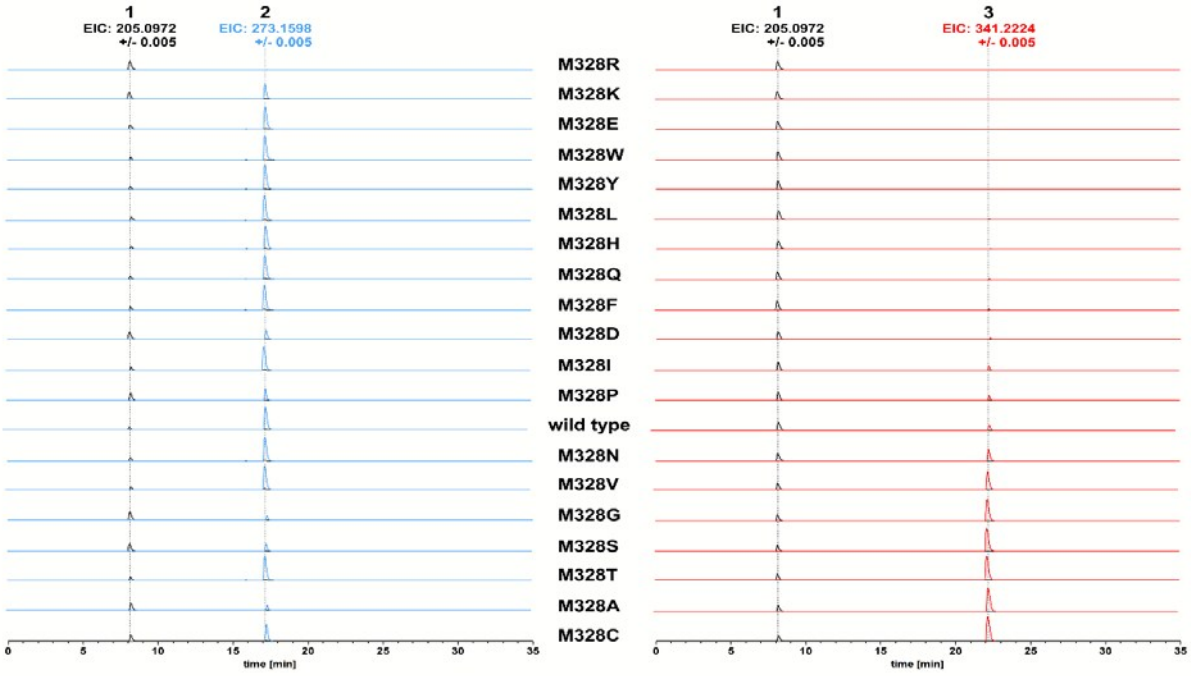

Fig. 2 Activities of FgaPT2 and M328 mutants toward DMAPP and GPP. The extracted ion chromatograms (EICs) of their incubation mixtures with **1** and DMAPP (blue) or GPP (red) are presented.

of Met328 seals the active site of the prenyl donor, closing the cavity from one side to form a hydrophobic pocket that is well suited to accommodate DMAPP. Any prenyl donor larger than DMAPP would clash with the bulky side chain of Met328. Altering this residue therefore represents an attractive strategy to enable the accommodation of GPP and FPP (Fig. 4).

Therefore, the mutant M328G was generated by site-directed mutagenesis and assayed with **1** in the presence of DMAPP, GPP or FPP under the same conditions as for FgaPT2. M328G showed a strongly reduced acceptance of DMAPP with a conversion of 6.0%.

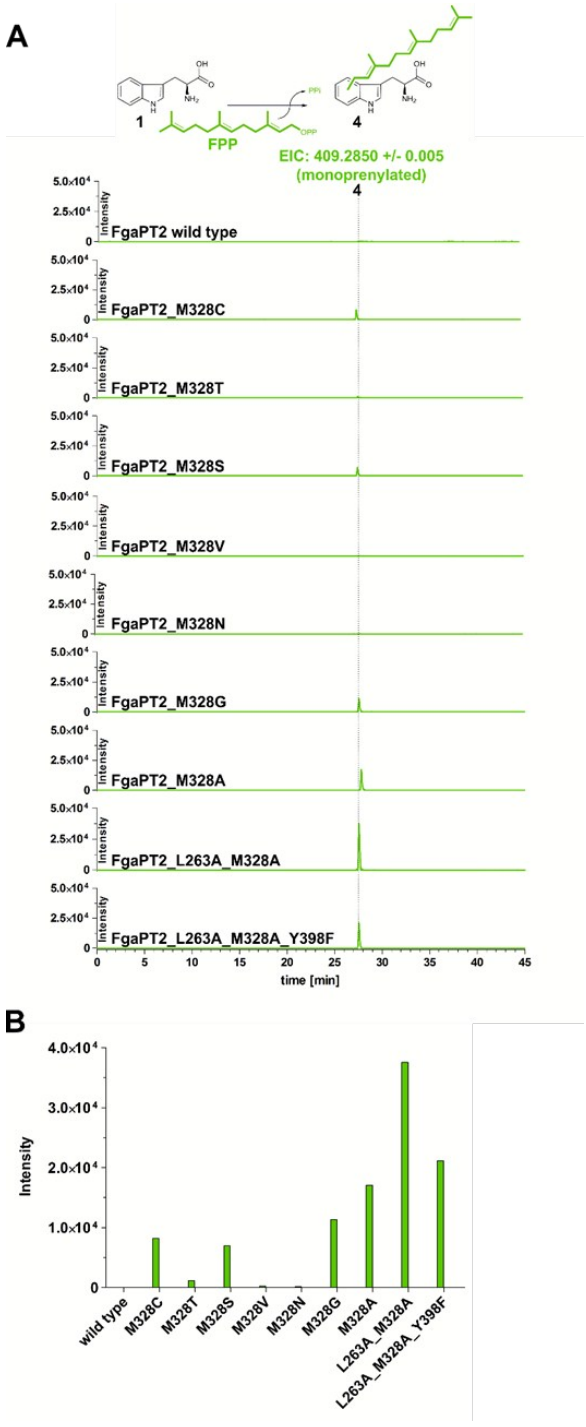

Fig.3 Farnesylation of L-tryptophan by FgaPT2 and mutants thereof. A) EICs and B) relative activities.

In contrast, it has an almost tenfold higher GPP acceptance than FgaPT2 (from 3.8% to 36.0%) (Figs. 1B and 2), highlighting the importance of Gly328 to reduce the steric hindrance for GPP-binding. Furthermore, a farnesylated product was clearly detected for M328G with FPP (Fig. 3). These results clearly identify residue 328 in FgaPT2 as a key residue for prenyl donor selectivity and the mutation of this residue to glycine enables an acceptance of GPP.

Comparison of the ternary crystal structure of FgaPT2 with those of FtmPT1[20] and CdpNPT[21] led to the identification of Met364 in FtmPT1 and Met349 in CdpNPT to be the corresponding residues of Met328 in FgaPT2. As the structures of 5-DMATS[24] and BrePT[25] are not available, we generated computational models on the basis of HHPRED[26] alignments and 3D modelling using MODELLER (https://salilab.org/modeller). Manual inspection of the superposition yielded the alignments illustrated in Figure 5. The corresponding gatekeeping residues were identified as Leu327 in 5-DMATS and Ile337 in BrePT, which are comparable in size to methionine. Mutation of the mentioned residues to glycine resulted in the formation of mutants with significantly increased activities towards GPP (data not shown).

Recently, the *Aspergillus terreus* prenyltransferase AtaPT was demonstrated to utilize various prenyl donors, with relatively low tolerance against DMAPP. The mutant AtaPT_G326M had lower acceptance for GPP and FPP, but it was more active towards DMAPP.[15] The reduced activity toward DMAPP by FgaPT2_M328G and AtaPT wild-type is unexpected initially, because these enzymes display a clear preference for prenyl donors longer than DMAPP. We conclude that, in addition to steric restraints, subtle changes in the active site can also have a major impact on the specificity. Mutation of Met328 in FgaPT2 to glycine increases the size of the active site cavity. As a result, the mobility of the dimethylallyl entity in the active site is increased during catalysis. This enables the prenyl donor to adopt slightly different conformations, which ultimately yield to a catalytic attack at different positions of the aromatic ring system. The resulting flexibility of the substrate DMAPP in the active site reduces therefore its activity for the reaction catalysed by the wildtype enzyme.

Structure elucidation of the new enzyme product 4-geranyltryptophan

For structure confirmation, the enzyme product 4-geranyltryptophan **3** was isolated from an up-scaled incubation mixture of M328G with **1** and GPP and subsequent subjected to NMR and MS analyses (Figs. S7 and S8). In the ^{1}H NMR spectrum, two characteristic signals appeared as broad triplets at δ_H 5.36 (1H) and 5.12 ppm (1H), confirming the regular attachment of the geranyl moiety with its C-1 atom. Additional signals from the geranyl moiety were observed at δ_H 3.81 (2H), 2.07-2.13 (4H), and those of the three methyl groups in the up-field region of δ_H 1.58-1.76 ppm (9H). Signals for four instead of five aromatic protons appeared in the down-field region, which verifies the prenylation at the indole ring. Comparison of the ^{1}H NMR spectrum of the GPP product (Fig. S7) with that of the *C4*-prenylated L-tryptophan **2**[19,27] revealed almost identical chemical shifts and coupling patterns for the four aromatic protons in both spectra, which unequivocally confirms the formation of 4-geranyltryptophan (**3**). These results clearly demonstrate that the targeted PT is redesigned from a 4-

View Article Online
DOI: 10.1039/C8OB02037J

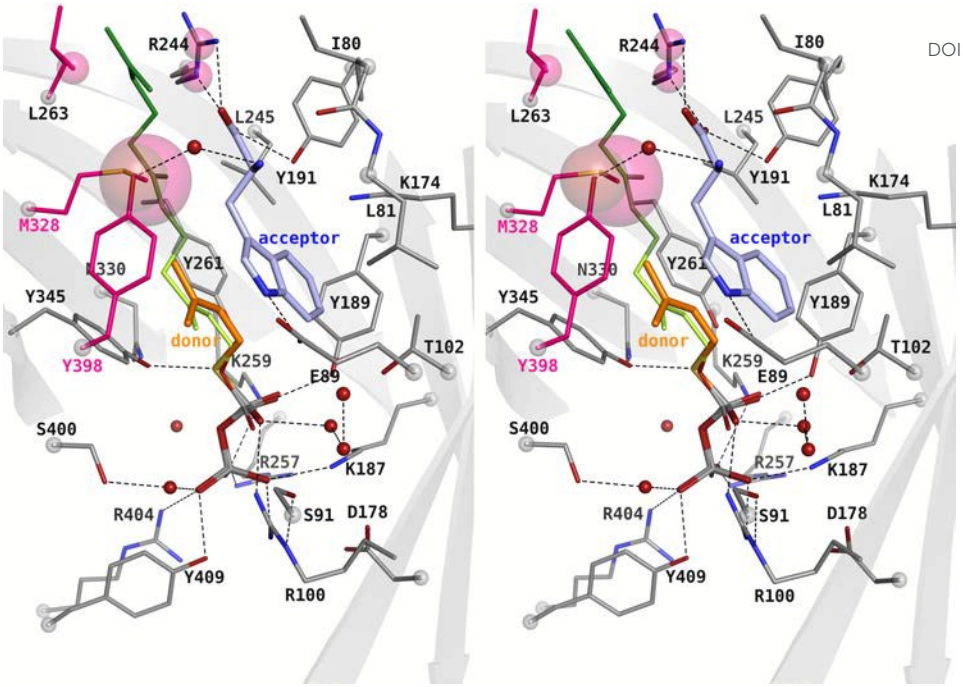

Fig.4 Model of FgaPT2 catalysis. GPP (light green) and FPP (dark green) were modelled into the crystal structure of FgaPT2 (pdb entry: 3I4X) with DMSPP (orange) after mutating M328 to glycine using FoldX. The isoprenoids are docked into the cavity on the basis of the DMAPP conformation. The pyrophosphate positions were kept fixed as the binding site, which is structurally conserved in all fungal prenyl transferases. Potential clashes between GPP/ FPP and the protein are indicated by spheres (pink). Smaller spheres indicate clashes that might be compensated by side chain reorientation. The closest distances to L263 and R244 are 2.8 Å and 3.0 Å, respectively.

dimethylallyltryptophan synthase to a 4-geranyltryptophan synthase by a single point mutation.

Position 328 in FgaPT2 controls the donor selectivity

As demonstrated above, Met328 in FgaPT2 is they gatekeeping residue for controlling the prenyl donor selectivity. This amino acid residue protrudes into the active centre, and it is therefore likely that steric effects prevent the acceptance of GPP and FPP (Fig. 4). Obviously, replacement of Met328 with glycine strongly decreased the steric hindrance, enabling the utilization of GPP and FPP for prenylations. The engineered enzyme also displays reduced activity toward DMAPP from 81.7% with FgaPT2 to 6.0% with M328G. The reduced activity indicates that beside steric restraints other molecular effects also influence the interaction with DMAPP. To uncover the molecular interactions between the prenyl donors and the key residue 328 in FgaPT2, we performed site-saturation mutagenesis to obtain mutants with the remaining 18 amino acids.

FgaPT2 and the nineteen M328X mutants were assayed with **1** in the presence of DMAPP, GPP or FPP and analysed via LC-MS (Fig. 2). Our results show that steric hindrance in the active centre is mainly responsible for the low GPP activity. The side chains of the mutants M328L, M328I, M328F, M328Q, and M328H are comparable in size to that of Met328 in the wild-type protein. These residues are located in the reaction cavity in a similar manner (Fig. 6) and therefore show catalytic activities as demonstrated for Met328. Absolute conversions of **1** were determined for these mutants in the range of 81.3-84.3% with DMAPP and of 0.4-3.3% with GPP (Fig. 1B). No product formation was detected with FPP.

Amino acid residues with smaller side chains than methionine (M328A, M328V, M328T, M328G, M328S, M328C, and M328N) show strongly enhanced catalytic activity toward GPP, with conversion rates in the range of 10.7-50.7% (Fig. 1B). Their acceptances for DMAPP differ substantially from each other, from nearly no changes in comparison to the wild type as in the cases of M328V, M328T, and M328N, to strongly reduced activities as in the cases of M328G, M328S, and M328A. Mutants M328T and M328C show similar enhanced activities for GPP and clear acceptance for DMAPP. M328C yielded the highest conversion of 50.7% with GPP. However, this mutant still exhibits a relatively high acceptance of DMAPP with a conversion of 40%. The best acceptance ratios of GPP to DMAPP were observed for M328G, M328S, and M328A, with conversions of 35.9, 42.9, and 47.1% for GPP and 6.0, 12.7, and 8.6% for DMAPP, respectively (Fig. 1B). Furthermore, the mutants with the smallest side chains, *i.e.* M328A, M328G, M328S, and M328C show a clear acceptance of FPP among the single mutants (Fig. 3).

The amino acid residues of M328T, M328V, and M328N would allow for the interaction with GPP, and their polar nature could also facilitate an interaction with DMAPP. As a consequence, mutants M328T, M328V, and M328N display a high acceptance for DMAPP with conversion rates of 81.2, 83.5, and 76.9%, respectively. This is comparable to the wild-type enzyme. However, they also show a high tolerance towards GPP with conversion rates of 44.6, 26.7, and 10.7%, respectively (Fig. 1B).

View Article Online
DOI: 10.1039/C8OB02037J

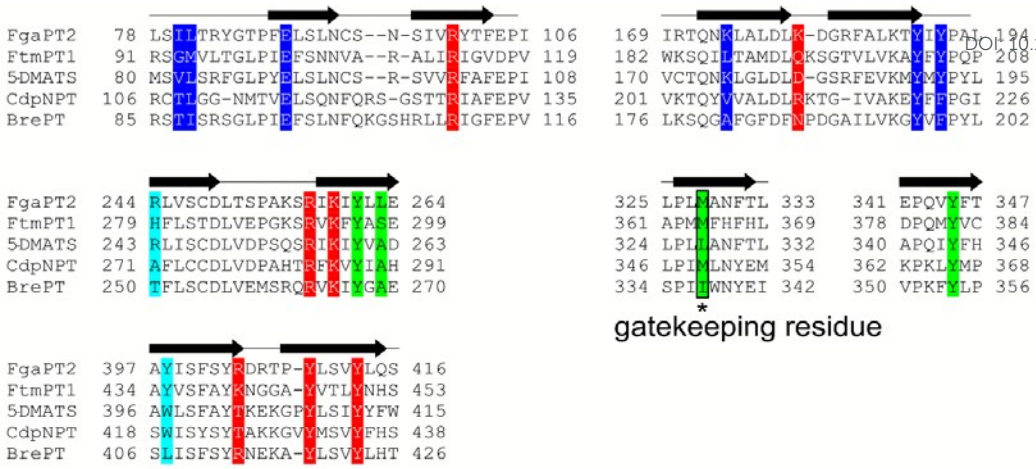

Fig. 5 Structure-based sequence alignments of five selected prenyltransferases. Labelled residues are suggested to be involved in the interactions with the pyrophosphate entity (red), the prenyl acceptor (blue, cyan) and dimethylallyl moiety (green). Residues corresponding to M328 of FgaPT2 are labelled with * (M, L, I).

The mutants M328Y, M328W, M328E, and M328K exhibit absolute conversions of 82.2, 77.4, 66.1, and 34.9% with DMAPP, respectively (Fig. 1B), and they are inactive toward GPP as well as FPP. The aromatic character of the side chains of M328Y and M328W probably explains the high activities of these mutants toward DMAPP. Although π-π-interactions to the prenyl donor seem impossible due to the perpendicular orientation of the π-systems, the aromatic side chains of M328W and M238Y interact perfectly with the hydrophobic and aliphatic character of DMAPP. On the other hand, the bulky side chains do not allow the incorporation of larger prenyl donors than DMAPP because of steric hindrance, likely preventing GPP and FPP from entering the reaction cavity or blocking the binding of the prenyl donor. These findings are in general agreement with the observed catalytic rates of the aromatic amino acid residues of M328F and M328H, which show similar activities toward DMAPP. Since the two side chains are less bulky in comparison to M328Y and M328W, they still display low acceptance of GPP. The acidic amino acid residue of M328E and the basic character of M328K significantly reduce the utilization of DMAPP (Fig. 1B). The amino acid residues proline and aspartic acid at 328 position revealed very similar behaviours toward the prenyl donors. They strongly reduced DMAPP and showed low GPP acceptance. The replacement of Met328 with arginine nearly abolished the acceptance of DMAPP, probably due to steric and polarity effects (Fig. 1B). We could not observe any activities for GPP or FPP with the M328R mutant.

In order to verify the geranylation position of **1** by M328S, M328A, M328C, M328T, M328V, and M328N mutants, the enzyme products were isolated and subjected to ^{1}H NMR analysis. Comparison of the spectra with that of **3** confirmed the same enzyme product in their reaction mixtures.

Site-saturation mutagenesis at position 328 in FgaPT2 revealed that the size of the amino acid residue at this position determines prenyl donor selectivity. However, polarity effects appear also crucial for binding DMAPP and GPP for prenyl transfer reactions. Molecular modelling (Figs. 4 and 6) revealed that any large and rigid amino acid side chain at position 328 would interfere with GPP prenylation, which is in agreement with our active site model. In contrast, high GPP conversions were found with very small side chain amino acids. M328A showed a high conversion yield of 47.1% with GPP and a low activity with DMAPP (8.6%) and therefore could

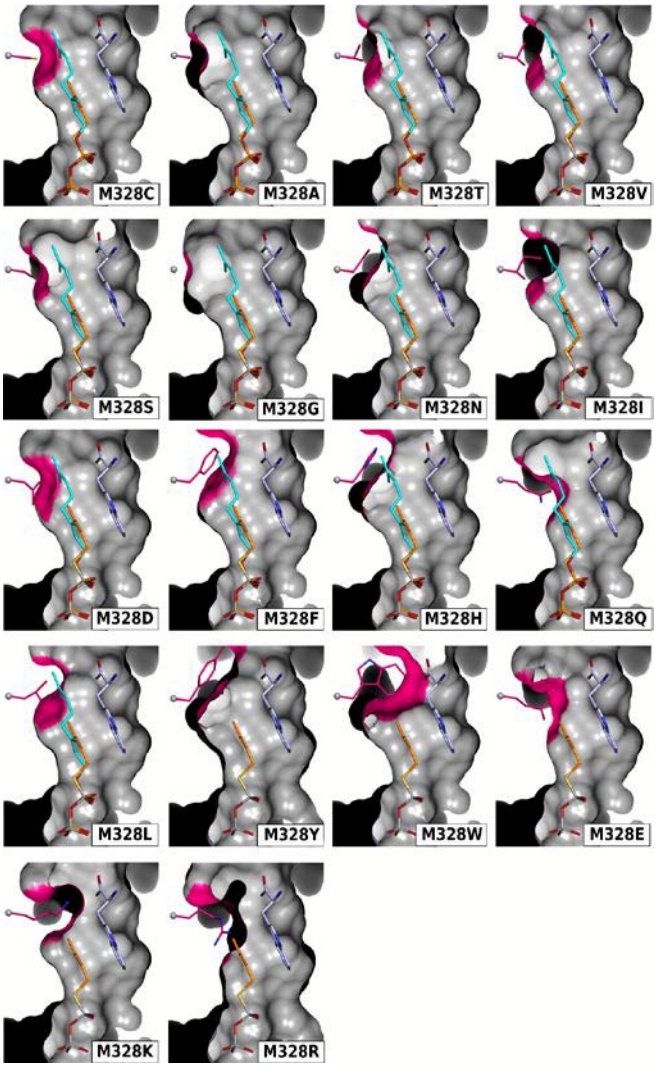

Fig.6 Mutations switching the specificity of FgaPT2 containing L-tryptophan (sky blue) from DMAPP (orange) to GPP (cyan). In silico models of selected FgaPT2 variants at position M328 (side chain shown in pink) emphasizing the importance of the gatekeeper residue for the acceptance of GPP and FPP. All FgaPT2 variants were calculated by FoldX. Mutant M328P is not shown as this mutant might interfere with the folding of the backbone. Large amino acid side chains would result in a clash with the prenyl entity thereby excluding GPP and FPP as prenyl donor. For DMAPP, the mutation to M328G seems to introduce too much flexibility in the active site thereby reducing the turnover.

be applied for *in vivo* production of specifically geranylated products in engineered organisms.

We conclude that, on the one hand, M328G, M328S, M328A, and M328C are particularly effective in reducing steric hindrance for GPP acceptance. On the other hand, they eliminate hydrophobic contacts that are crucial for optimal fitting of DMAPP. The alanine residue of M328A provides the second highest conversion of 47.1% with GPP and the second lowest activity with DMAPP (8.6%) of the mutants that can utilize GPP. To the best of our knowledge, this catalytic behaviour is unique, because M328A offers enough space and hydrophobic interactions for optimal GPP and FPP binding and therefore also shows the highest acceptance for FPP (Fig. 3). It appears that the increased size of the active site in the mutant introduces a higher degree of substrate mobility for the small dimethylallyl entity inside the reaction chamber. This likely hampers the correct positioning of the prenyl acceptor and yields to a decreased *C4*-prenylation.

The influence of polarity effects that distinguish between DMAPP and GPP can be verified through a comparison of the reactivity of M328V with M328T, and that of M328S with M328C. Despite the equal size of the side chains of M328T and M328V, M328T exhibits a significantly higher conversion rate with GPP than M328V, whereas the DMAPP acceptance is for both enzymes comparable. The two amino acid residues differ only in their substitutions at the β-carbon. The hydroxyl group at β-carbon of M328T enhances GPP turnover in comparison of the methyl group at the β-carbon of M328V. The amino acids in M328S and M328C differ also in their substitutions at the β-carbon. Considering the observed conversions, the thiol group in M328C and the hydroxyl group in M328S show similar effects on their acceptance for GPP, but differ significantly in their DMAPP catalysis. Polarity effects appear also crucial for binding DMAPP and GPP for prenyl transfer reactions. The side chain of M328C and M328S differ only slightly in their size. The atom radii are 66 for oxygen and 104 pm for sulphur, respectively. But the softer character of the thiol group possessing a polarizable electron shell can compensate for the increased cavity size of the active centre that yielded to a decreased DMAPP turnover by variant M328S, thereby enhancing the DMAPP turnover in M328C.

Determination of kinetic parameters

To obtain insights into the catalytic efficiency, Michaelis-Menten kinetic of FgaPT2 and seven mutants with the best acceptance for GPP (M328C, M328A, M328T, M328S, M328G, M328V, and M328N) (Fig. S9) were determined by using the software GraphPad Prism 5.0 by a nonlinear regression. As given in Table 1, these mutants exhibit K_M values for GPP in the range of 0.078 – 0.48 mM and turnover numbers (k_{cat}) in the range of 0.0037 – 0.11 s^{-1}. The calculated catalytic efficiencies (k_{cat}/K_M) in the range of 181 – 317 s^{-1} M^{-1} are comparable for the first five mutants. Significantly lower catalytic efficiencies were observed for M328V and M328N with GPP. These results are in good agreement with those presented in Fig. 1B.

In summary, absolute conversion yields of up to 50%, i.e. 50-60% of that of wild type with DMAPP, were detected with five mutants (Fig. 1B). The turnover number of the best mutant towards GPP was determined at 0.11 s^{-1}, *i.e.* 25 % of that of the wild type enzyme with DMAPP. The *kcat*/*KM* values of the mutants for GPP are, however, significantly lower than that of the wild type with DMAPP. This is due to the extremely unusual low *KM* value of the wild type enzyme towards DMAPP at 4 µM, although the *KM* values of the mutants with GPP are in the normal range of many secondary metabolite enzymes. Therefore, the obtained mutants can be considered as effective biocatalyst.

Table 1. Kinetic parameters of FgaPT2 and mutants toward DMAPP and GPP in the presence of **1**.

enzyme	k_M [mM]	k_{cat} [s^{-1}]	k_{cat}/k_M [s^{-1} M^{-1}]
	DMAPP		
FgaPT2 wild type	0.0040	0.44	110000
	GPP		
FgaPT2_M328C	0.48	0.11	229
FgaPT2_M328A	0.20	0.050	250
FgaPT2_M328T	0.31	0.056	181
FgaPT2_M328S	0.18	0.057	317
FgaPT2_M328G	0.12	0.032	267
FgaPT2_M328V	0.13	0.0095	73
FgaPT2_M328N	0.078	0.0037	47

Enhancing farnesylation activity

Our saturation mutagenesis results on M328 demonstrate that this key residue is crucial to turn on the GPP and FPP activity (Figs. 1–3). The low turnover observed for FPP indicates that additional amino acid residues are also involved in FPP-binding. Molecular modelling revealed that Leu263 and Tyr398 could contribute as additional positions to FPP-activity (Fig. 4). The modelling shows that these amino acids most likely sterically interfere with the terminal isoprenyl entity of FPP. As a side effect, this might hamper the accommodation of the prenyl acceptor in the binding site. We therefore mutated them to amino acids bearing smaller side chains. As M328A has the highest activity toward FPP, we chose this mutant for further mutagenesis experiments and created L263A_M328A as double and L263A_M328A_Y398F as triple mutant. Both engineered enzymes have increased activity toward DMAPP (approximately 15%) and simultaneously decreased activity toward GPP (also 15%), compared to M328A. Clear enhancement of the activity towards FPP was observed for the double (1.4%) and triple mutant (1.1%), in comparison to 0.7% with M328A and no product formation with FgaPT2 (Fig. 3).

Although our model shows that farnesylation would be possible by the mutation of the gatekeeping residue M328 in FgaPT2 to glycine, the turnover rates remain low for this bulky prenyl donor. Plausible reasons for this observation are difficulty for the hydrophobic and long FPP molecule to enter the active site, and steric pressure at the end of the prenyl tail with the residues R244, L263 or Y398. Additionally, it seems possible that the very long tail

of the prenyl donor might interact with the correct position of the prenyl acceptor, thereby reducing the enzyme activity with the FPP substrate. Through the mutation of a second residue, L263A, we are able to achieve a product yield of 1.4% with **1** and FPP with L263A_M328A. While this reaction rate is obviously too low for the use of the double mutant as a farnesyltransferase, it still shows that our design has potential because wild-type FgaPT2 does not accept FPP at all.

Experimental

Chemicals and strains

DMAPP, GPP and FPP were synthesized according to the procedure described for GPP by Woodside et al.[23] 1-Chloro-3-methyl-2-butene, geranyl chloride, or farnesyl chloride in acetonitrile was stirred with tris(tetrabutyl ammonium) hydrogen pyrophosphate at room temperature for 2 h. After removal of the tetrabutyl ammonium salt by passing over a Dowex AG 50W-X8 column, the resulted prenyl diphosphate was extracted with a mixture of acetonitrile:2-propanol (1:1) and ammonium bicarbonate (0.05M). The supernatants were combined and the organic solvents were removed with a rotary evaporator under reduced pressure. The aqueous residue was subsequently lyophilized. L-tryptophan was purchased from Roth (Karlsruhe, Germany). *E.coli* XL1-Blue MRF´ (Stratagene) and BL21(DE3) pLysS (Invitrogen, Karlsruhe, Germany) were used for propagation of transformed plasmids, and overproduction of recombinant proteins, respectively. Terrific Broth medium supplemented with 50µg/mL carbenicillin or 25 µg/mL kanamycin was used for cultivation of recombinant *E.coli* strains. Primer sequences used in this study are listed in Table S1.

Site-directed and site-saturation mutagenesis

The plasmid harboring *fgaPT2* was applied as DNA template for mutagenesis by PCR. To obtain specific or all variants of mutations at desired gene position, (degenerated) primers were designed as described by the optimized site-directed mutagenesis protocols[28,29] and synthesized by Eurofins Genomics GmbH (Ebersberg, Germany) or Seqlab GmbH (Göttingen, Germany). Expand Long Template PCR System (Roche Diagnostics GmbH, Mannheim) was used for PCR amplification. An annealing temperature of 62 °C and elongation time of 8 min for *fgaPT2* was adjusted to the thermal profile.

Heterologous overexpression and purification of recombinant proteins

The recombinant histidine-tagged PT His_8-FgaPT2 as well as the corresponding engineered proteins were overproduced in *E.coli* and purified by Ni-NTA affinity chromatography (Qiagen, Hilden) according to published procedure.[27] Protein concentrations were measured at 280 nm with NanoDrop 2000c UV-VIS spectrophotometer setting proteins specific extinction coefficient and molecular weight. To ensure accurate concentration, proteins were further analysed on SDS-PAGE. Intensities of the Coomassie stained proteins were compared with those of the standardized markers.

Enzyme activity assays

Each reaction mixture contained 10 µg of purified recombinant protein, 1.0 mM of **1**, 1.0 mM DMAPP, GPP or FPP as prenyl donor, 10 mM $CaCl_2$, up to 10% (v/v) glycerol, and up to 5% (v/v) DMSO. All enzyme assays were performed in duplicate adjusting with 50 mM Tris-HCl (pH 7.5) to a total volume of 50 µL. After careful mixing, the reactions were incubated at 37 °C for 90 min, stopped with an equal volume of methanol and vortexed vigorously. Before injecting to LC-MS, mixtures were centrifuged at 13,300 rpm for 20 min to yield a clear supernatant.

LC-MS analysis

A sample volume of 5 µL was injected and analysed on an Agilent HPLC 1260 series system (Agilent Technologies, Böblingen, Germany) connected to a Bruker microTOF QIII mass spectrometer with ESI-source (Bruker, Bremen, Germany). Agilent Eclipse XDB-C18, 5 µm, 4.6x150 mm column was used for separation of the enzyme products. Solvent A (H_2O) and solvent B (MeCN), both adjusted to 0.1% formic acid, were run with a flow rate of 0.5 mL/min and a linear gradient from 5% to 100% of solvent B over 40 min for analysing prenylated products. The column was washed for 5 min with 100% B prior equilibrating for further 5 min to the initial solvent composition of 5% B and 95% A. Electrospray ionization positive ion mode was selected for determining the masses. Sodium formate was used in each run for mass calibration. The masses were scanned in the range of 100-1500 m/z. The capillary voltage was set to 4.5 kV and a collision energy of 8.0 eV. Data were evaluated with the Compass Data Analysis 4.2 software (Bruker Daltonik, Bremen, Germany).

Upscaling enzyme reactions and HPLC-based product isolation

Structure elucidation *via* ^{1}H NMR needed an upscaling of the enzyme reactions to a total volume of up to 7.0 mL. The appropriate product amount was achieved with enzyme assays containing 1.0 mM of **1**, 2.0 mM DMAPP or GPP, 10 mM $CaCl_2$, up to 10% (v/v) glycerol, up to 5.0% (v/v) DMSO, 50 mM Tris HCl (pH 7.5), and up to 1.38 mg of purified recombinant proteins. The reaction mixtures were slightly agitated at 37 °C for 16 h. Equal volume of methanol was added to the incubation mixtures to terminate the reactions with a subsequent vigorously mixing for several minutes. To remove protein, a centrifugation step followed with 6,000 rpm for 20 min. The clear supernatant was transferred to a pear shaped flask and evaporated to dryness and dissolved in appropriate volume of DMSO and/or methanol. Prior to isolation via HPLC, the samples were centrifuged at 13,300 rpm for 20 min. The prenylated products were isolated on an Agilent HPLC 1200 series system (Böblingen, Germany) equipped with a semi-preparative Agilent ZORBAX Eclipse XDB C18 HPLC column (9.4 x 250 mm, 5 µm) at a flow rate of 2.5 mL/min. A linear gradient from 40% to 100% MeCN over 40 min was run to isolate the geranylated **3**.

NMR analysis

The isolated product was dissolved in CD_3OD and measured on a JEOL ECA-500 MHz spectrometer (JEOL Germany GmbH, Munich, Germany). The recorded ^{1}H NMR spectrum was processed and evaluated using MestReNova Version: 6.0.2-5475 software (Mestrelab Research S.L.). As internal reference, the solvent signal was set at 3.31 ppm, respectively.

^{1}H NMR data of **3** in CD_3OD: δ_{ppm} (multi, Hz) 7.20 (dd, 8.1, 0.7, 1H), 7.16 (s, 1H), 7.00 (dd, 8.1, 7.3, 1H), 6.81 (dd, 7.3, 0.7, 1H), 5.36 (tq, 6.9, 1.2, 1H), 5.12 (tsept, 6.9, 1.3, 1H), 3.81 (m, 4H, overlapping

with solvent signals), 3.14 (m, 1H), 2.13 (m, 2H), 2.07 (m, 2H), 1.76 (d, 0.8, 3H), 1.65 (d, 1.0, 3H), 1.58 (d, 0.6, 3H).

Determination of kinetic parameters

Kinetic parameters were determined by incubation of an appropriate amount of purified recombinant FgaPT2 or mutant with 1 mM of **1** and varied concentrations of DMAPP or GPP as prenyl donors at 37 °C. An optimal protein amount and incubation time were determined by measuring protein and time dependency. The enzyme assays were performed in duplicate. Protein concentration of 0.1 µM for FgaPT2 and an incubation time of 2 min were applied to determine the enzyme kinetics for DMAPP. To determine the kinetic parameters of FgaPT2 mutants for GPP, 1.9 µM of M328X (X = C, A, T, S, G and V) and 3.8 µM of M328N were incubated for 20 min. In a total volume of 50 µL, each reaction mixture contained DMAPP or GPP in concentrations of up to 0.5 or 1.0 mM, 1.0 mM of **1**, 10 mM $CaCl_2$, up to 3.6% (v/v) glycerol, and 50 mM Tris-HCl (pH 7.5). The reactions were terminated with 50 µL MeOH and subsequently centrifuged at 13,300 rpm for 20 min. A volume of 80 µL supernatant was injected and analysed by HPLC.

Molecular modelling and docking

The conformations of the mutants were calculated in silico using foldx.[30,31] Substrate docking was done manually for GPP and FPP using COOT[32] and DMAPP of FgaPT2 (PDB code: 3I4X) as a template. The conformation of the prenyl donors were energetically optimized. Docking of **1** was performed by in silico docking using vina.[33] The possible docking poses were analysed and verified for chemical sense of the observed catalytic reaction. Figures were generated with pymol (The PyMOL Molecular Graphics System, Version 1.8 Schrödinger, LLC.).

Conclusions

In summary, we demonstrated a convenient approach to obtain modified enzymes in which the substrate specificities differ clearly from the wild-type enzyme and from each other. By structure-based modelling of the tryptophan *C4*-dimethylallyl transferase FgaPT2, we are able to increase GPP and FPP acceptance by the mutation of gatekeeping residues. To the best of our knowledge, a natural or unnatural geranyl transferase or farnesyltransferase for tryptophan as a free amino acid has not been reported prior to this study. Our results provide evidence that a switch of the prenyl donor acceptance is not only possible for enzymes with high flexibility for these substrates such as AtaPT, MpnD and TleC,[15,16] but can also be applied for enzymes which are practically limited to the use of DMAPP as donor. Several mutants show high activity towards GPP and could already be used as geranyl transferases for chemoenzymatic synthesis and synthetic biology. Our findings should encourage the PT community to manipulate additional ones of the approximately 45 DMATS-type PTs, which mainly use DMAPP as prenyl donor.[5] The farnesyltransferase activities are necessary to be optimized by identification of other important factors and additional mutations. This would require additional structural data, *e. g.* of the engineered enzymes.

Conflicts of interest

View Article Online
DOI: 10.1039/C8OB02037J

The authors declare no competing financial interest.

Acknowledgements

We thank Wolfgang Brandt (IPB, Halle) for suggestions, Lena Ludwig-Radtke, Rixa Kraut, Stefan Newel (University of Marburg) for synthesis of prenyl donors, taking MS and NMR spectra, respectively.

Funding information The Bruker micrOTOF QIII mass spectrometer was financially supported in part by a grant from the Deutsche Forschungsgemeinschaft (INST 160/620-1 to S.-M. L.).

Notes and references

1 G. F. Bills and J. B. Gloer, *Microbiol Spectr.*, 2016, **4**, 1-32.
2 D. J. Newman and G. M. Cragg, *J. Nat. Prod.*, 2016, **79**, 629-661.
3 J. Bérdy, *J. Antibiot.*, 2012, **65**, 441.
4 C. T. Walsh and M. A. Fischbach, *J. Am. Chem. Soc.*, 2010, **132**, 2469-2493.
5 J. Winkelblech, A. Fan, and S.-M. Li, *Appl. Microbiol. Biotechnol.*, 2015, **99**, 7379-7397.
6 M. Wang and P. J. Casey, *Nat. Rev. Mol. Cell Biol.*, 2016, **17**, 110-122.
7 F. Tsuji, A. Ishihara, K. Kurata, A. Nakagawa, M. Okada, S. Kitamura, K. Kanamaru, Y. Masuda, K. Murakami, K. Irie, and Y. Sakagami, *FEBS Lett.*, 2012, **586**, 174-179.
8 M. Okada, I. Sato, S. J. Cho, H. Iwata, T. Nishio, D. Dubnau, and Y. Sakagami, *Nature Chem. Biol.*, 2005, **1**, 23-24.
9 C. E. Dumelin, Y. Chen, A. M. Leconte, Y. G. Chen, and D. R. Liu, *Nat. Chem. Biol.*, 2012, **8**, 913-919.
10 W. Xu, D. J. Gavia, and Y. Tang, *Nat. Prod. Rep.*, 2014, **31**, 1474-1487.
11 S.-M. Li, *Nat. Prod. Rep.*, 2010, **27**, 57-78.
12 T. Kuzuyama, J. P. Noel, and S. B. Richard, *Nature*, 2005, **435**, 983-987.
13 U. Metzger, C. Schall, G. Zocher, I. Unsöld, E. Stec, S.-M. Li, L. Heide, and T. Stehle, *Proc. Natl. Acad. Sci. U. S. A*, 2009, **106**, 14309-14314.
14 Y. H. Chooi, P. Wang, J. Fang, Y. Li, K. Wu, P. Wang, and Y. Tang, *J. Am. Chem. Soc.*, 2012, **134**, 9428-9437.
15 R. Chen, B. Gao, X. Liu, F. Ruan, Y. Zhang, J. Lou, K. Feng, C. Wunsch, S.-M. Li, J. Dai, and F. Sun, *Nat. Chem. Biol.*, 2017, **13**, 226-234.
16 T. Mori, L. Zhang, T. Awakawa, S. Hoshino, M. Okada, H. Morita, and I. Abe, *Nat. Commun.*, 2016, **7**, 10849.
17 D. Pockrandt, C. Sack, T. Kosiol, and S.-M. Li, *Appl. Microbiol. Biotechnol.*, 2014, **98**, 4987-4994.
18 S. Tarcz, X. Xie, and S.-M. Li, *RSC Adv.*, 2014, **4**, 17986-17992.
19 I. A. Unsöld and S.-M. Li, *Microbiology*, 2005, **151**, 1499-1505.
20 M. Jost, G. Zocher, S. Tarcz, M. Matuschek, X. Xie, S.-M. Li, and T. Stehle, *J. Am. Chem. Soc.*, 2010, **132**, 17849-17858.
21 J. M. Schuller, G. Zocher, M. Liebhold, X. Xie, M. Stahl, S.-M. Li, and T. Stehle, *J. Mol. Biol.*, 2012, **422**, 87-99.
22 X. Yu, G. Zocher, X. Xie, M. Liebhold, S. Schütz, T. Stehle, and S.-M. Li, *Chem. Biol.*, 2013, **20**, 1492-1501.
23 A. B. Woodside, Z. Huang, and C. D. Poulter, *Org. Synth.*, 1988, **66**, 211-215.

View Article Online
DOI: 10.1039/C8OB02037J

24 X. Yu, Y. Liu, X. Xie, X.-D. Zheng, and S.-M. Li, *J. Biol. Chem.*, 2012, **287**, 1371-1380.
25 S. Yin, X. Yu, Q. Wang, X. Q. Liu, and S.-M. Li, *Appl. Microbiol. Biotechnol.*, 2013, **97**, 1649-1660.
26 J. Söding, A. Biegert, and A. N. Lupas, *Nucleic Acids Res.*, 2005, **33**, W244-W248.
27 N. Steffan, I. A. Unsöld, and S.-M. Li, *Chembiochem*, 2007, **8**, 1298-1307.
28 H. Liu and J. H. Naismith, *BMC. Biotechnol.*, 2008, **8**, 91.
29 L. Zheng, U. Baumann, and J. L. Reymond, *Nucleic Acids Res.*, 2004, **32**, e115.
30 J. W. Schymkowitz, F. Rousseau, I. C. Martins, J. Ferkinghoff-Borg, F. Stricher, and L. Serrano, *Proc. Natl. Acad. Sci. U. S. A*, 2005, **102**, 10147-10152.
31 J. Schymkowitz, J. Borg, F. Stricher, R. Nys, F. Rousseau, and L. Serrano, *Nucleic Acids Res.*, 2005, **33**, W382-W388.
32 P. Emsley, B. Lohkamp, W. G. Scott, and K. Cowtan, *Acta Crystallogr. D. Biol. Crystallogr.*, 2010, **66**, 486-501.
33 O. Trott and A. J. Olson, *J. Comput. Chem*, 2010, **31**, 455-461.